Domain wall mobility in nanowires: Transverse versus vortex walls

R. Wieser, U. Nowak, and K. D. Usadel
Theoretische Tieftemperaturphysik, Gerhard-Mercator-Universität Duisburg, 47048 Duisburg, Germany
(Received 12 May 2003; revised manuscript received 30 October 2003; published 11 February 2004)

The motion of domain walls in ferromagnetic, cylindrical nanowires is investigated numerically by solving the Landau-Lifshitz-Gilbert equation for a classical spin model in which energy contributions from exchange, crystalline anisotropy, dipole-dipole interaction, and a driving magnetic field are considered. Depending on the diameter, either transverse domain walls or vortex walls are found. The transverse domain wall is observed for diameters smaller than the exchange length of the given material. Here, the system behaves effectively one dimensional and the domain wall mobility agrees with a result derived for a one-dimensional wall by Slonczewski. For low damping the domain wall mobility decreases with decreasing damping constant. With increasing diameter, a crossover to a vortex wall sets in which enhances the domain wall mobility drastically. For a vortex wall the domain wall mobility is described by the Walker formula, with a domain wall width depending on the diameter of the wire. The main difference is the dependence on damping: for a vortex wall the domain wall mobility can be drastically increased for small values of the damping constant up to a factor of $1/\alpha^2$.

DOI: 10.1103/PhysRevB.69.064401 PACS number(s): 75.10.Hk, 75.40.Mg, 75.60.Ch

Arrays of magnetic nanowires are possible candidates for patterned magnetic storage media.[1,2] For these nanowires and also for other future magnetoelectronic devices the understanding of domain wall motion and mobility is important for the controlled switching of the nanostructure. In a recent experiment, the velocity of a domain wall in a NiFe/Cu/NiFe trilayer was investigated using the giant magneto-resistance (GMR) effect.[3] The measured velocities were compared with the Landau-Lifshitz formula for domain wall motion.[4] This comparison was used to determine the damping constant of the trilayer, a quantity that is usually not known *a priori*. However, several formulas for the velocity of a domain wall can be found in the literature[4–8] which are derived in different limits and all in (quasi-) one-dimensional models, neglecting the possible influence of nonuniform spin structures within the domain wall. Thus the question arises in how far these formulas are applicable to real three-dimensional domain structures. To shed some light onto this problem, we numerically investigate the domain wall mobility in nanowires starting from a three-dimensional local spin model.

In the following we consider a classical spin model with energy contributions from exchange, crystalline anisotropy, dipole-dipole interaction, and a driving magnetic field. Such a spin model for the description of magnetic nanostructures[9] can be justified following different lines: on the one hand, it is the classical limit of a quantum-mechanical, localized spin model; on the other hand, it might be interpreted as the discretized version of a micromagnetic continuum model, where the charge distribution for a single cell of the discretized lattice is approximated by a point dipole. For certain magnetic systems their description in terms of a lattice of magnetic moments may even be based on the mesoscopic structure of the material, especially when a particulate medium is described.

However, our intention is not to describe a particular material but to investigate a general model Hamiltonian, which is

$$\mathcal{H}=-J\sum_{\langle ij\rangle}\mathbf{S}_i\cdot\mathbf{S}_j-\mu_s\mathbf{B}\cdot\sum_i\mathbf{S}_i-D_e\sum_i(S_i^z)^2$$
$$-\omega\sum_{i<j}\frac{3(\mathbf{S}_i\cdot\mathbf{e}_{ij})(\mathbf{e}_{ij}\cdot\mathbf{S}_j)-\mathbf{S}_i\cdot\mathbf{S}_j}{r_{ij}^3},\qquad(1)$$

where the $\mathbf{S}_i=\boldsymbol{\mu}_i/\mu_s$ are three-dimensional magnetic moments of unit length on a cubic lattice.

The first sum is the ferromagnetic exchange between nearest neighbors with coupling constant J. The second sum is the coupling of the spins to an external magnetic field B, the third sum represents a uniaxial anisotropy, here, with $D_e>0$, favoring the z axis as the easy axis of the system, and the last sum is the dipolar interaction where $w=\mu_0\mu_s^2/(4\pi a^3)$ describes the strength of the dipole-dipole interaction. The $\mathbf{e}_{ij}$ are unit vectors pointing from lattice site i to j and r_{ij} is the distance between these lattice sites in units of the lattice constant a.

The underlying equation of motion for magnetic moments, which we consider in the following, is the Landau-Lifshitz-Gilbert (LLG) equation,

$$\frac{\partial\mathbf{S}_i}{\partial t}=-\frac{\gamma}{(1+\alpha^2)\mu_s}\mathbf{S}_i\times[\mathbf{H}_i(t)+\alpha(\mathbf{S}_i\times\mathbf{H}_i(t))],\qquad(2)$$

with the gyromagnetic ratio $\gamma=1.76\times10^{11}\ (\mathrm{T\,s})^{-1}$, the dimensionless damping constant α (after Gilbert), and the internal field $\mathbf{H}_i(t)=-\partial\mathcal{H}/\partial\mathbf{S}_i$.

In the following we present results from the simulation of cylindrical systems being parallel to the z axis with a length of 256 lattice sites (except for Fig. 6 where results for a system size of 500 lattice sites are shown) and different diameters d. Our systems are defined on a cubic lattice and consist of dipoles at those lattice sites which reside within the cylinder of given diameter and length. Due to shape as well as crystalline anisotropy the equilibrium magnetization is aligned with the long axis of the system. However, we start

 ©2004 The American Physical Society

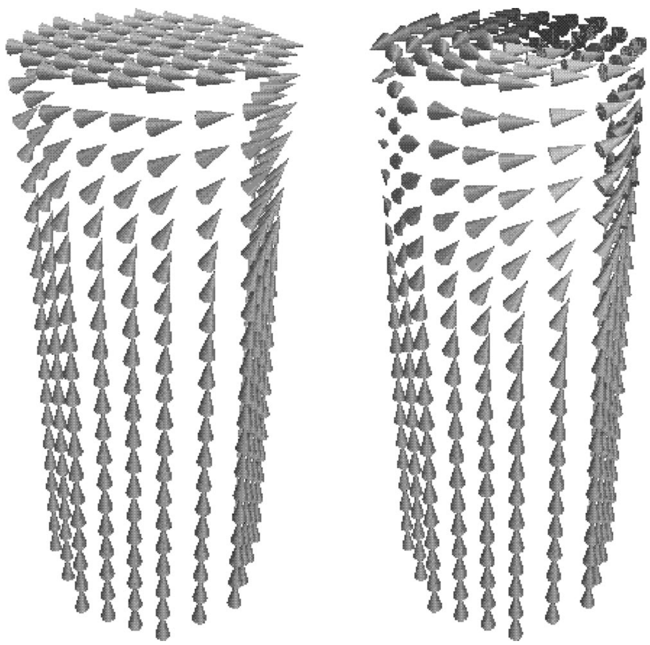

FIG. 1. Snapshots of a transverse (left, $\omega/J=0.003$) and a vortex (right, $\omega/J=0.2$) wall. The diameter $d=8$ is kept constant while the exchange length of the system is varied. Shown is only a part of the system below the current wall position. $D_e/J=0.05$.

the simulation with an abrupt, head-to-head domain wall as initial configuration, letting the wall relax until a stable state is reached. The distance of the initial wall position from the end is $\approx 1/3$ of the system length. Then we switch on the driving magnetic field B along the easy axis and wait until a stationary state is reached for some time interval in which the velocity v of the wall is constant while the wall is moving through the central part of the wire. We calculate the domain wall velocity from the magnetization versus time data, averaged over a period of time where no influence of the finite system size on the domain wall can be observed, i.e., until the wall approaches the other end of the wire.

Inspection of the stationary state of the moving domain wall shows that, depending on the ratio ω/J, either transverse domain walls or vortex walls are found. Representative spin configurations are shown in Fig. 1 for the static limit $(B=0)$. The transverse domain wall (left hand side) is observed for diameters smaller than the exchange length $d_{ex}/a=\pi\sqrt{J/[6\omega\zeta(3)]}$ of the system,[10] where $\zeta(3)\approx 1.2$ is Riemann's Zeta function [see also Ref. 11 for the exchange length in continuum theory where $3\zeta(3)$ is replaced by π]. Here all spins within cross-sectional planes perpendicular to the wire axis are parallel so that the system is effectively one dimensional. Note, that the spin precession leads to a rotation of the spin direction within the wall while it is moving.

With increasing dipolar interaction, a crossover to a vortex wall sets in (right-hand side of Fig. 1), which is now energetically favorable since the vortex structure leads to a flux closure. These findings are in agreement with corresponding spin model simulations of thermally activated reversal[10] and micromagnetic results[12,13] obtained from simulations of the LLG equation using a micromagnetic continuum model.

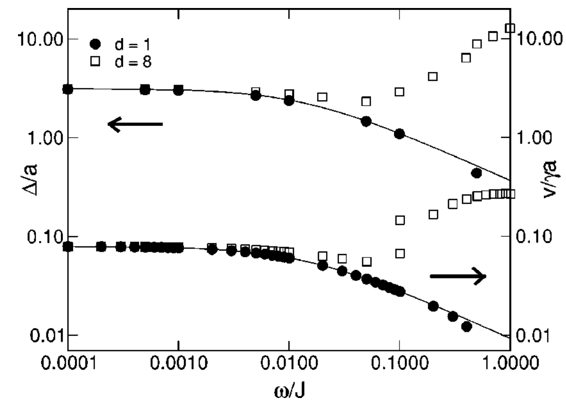

FIG. 2. Domain wall velocity and domain wall width vs dipolar coupling for a spin chain and a cylindrical system, respectively. $D_e/J=0.05$, $\mu_s B/J=0.05$, $\alpha=1$. The solid lines correspond to Eqs. (4) and (3); error bars are smaller than the symbol size.

In the following we turn to the investigation of the influence of the domain wall width and structure on its velocity. Figure 2 compares the dependence of the domain wall width Δ and domain wall velocity v on the strength of the dipolar coupling. Here, the domain wall width was determined numerically by fitting a tanh profile to the easy-axis magnetization of the moving wall in the stationary state where the magnetization is averaged over cross-sectional planes. However, it should be mentioned that for large dipolar interaction in a vortex wall the wall profile cannot accurately be described by a simple tanh profile. Note, that even in the limit $\omega\rightarrow 0$ the wall is stabilized by the additional crystalline anisotropy D_e.

For a spin chain $(d=1)$ the domain wall is necessarily always planar while for the system with a larger diameter a crossover to a vortex wall occurs. The crossover can be identified as a jump of the domain wall velocity for the $d=8$ data. Figure 2 demonstrates that for a transverse wall the domain wall velocity is proportional to the wall width. For a vortex wall this is at least qualitatively the case. Widths and velocities of transverse walls decrease with increasing dipolar interaction while for vortex walls the opposite is true. The crossover itself leads to a jump of the wall velocity not the wall width.

For a transverse wall the domain wall velocity is well described by an equation derived by Slonczewski as the lower limit for one-dimensional domain wall motion,[5]

$$v=\frac{\gamma}{\alpha+1/\alpha}\Delta_B B. \tag{3}$$

Here, Δ_B is the well-known Bloch wall width,

$$\Delta_B=a\sqrt{\frac{J}{2[D_e+3\omega\zeta(3)]}}, \tag{4}$$

where, for our case, the denominator $D_e+3\omega\zeta(3)$ estimates the effective anisotropy coming from shape as well as crystalline contributions [as before in a continuum theory $3\zeta(3)$ is replaced by π]. Both the above equations are drawn in

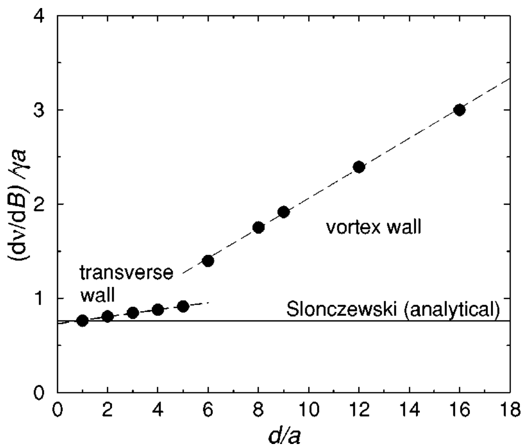

FIG. 3. Domain wall mobility vs diameter of cylindrical systems. The model parameters are $\omega/J=0.003$, $D_e/J=0.1$, $\alpha=1$. The constant line corresponds to Eq. (3); the dashed lines are guides to the eye. Error bars are smaller than the symbol size.

Fig. 2 as solid lines and they agree very well with the numerical data for transverse walls.

In the following we focus on the mobility of vortex walls. The crossover from the transverse to the vortex wall can also be observed while varying the diameter of the system, keeping the exchange length constant. Since for sufficiently small driving fields the domain wall velocity is proportional to the field in Fig. 3 we directly show the domain wall mobility dv/dB versus the diameter of the system. Obviously there are two distinct regions with distinct wall mobility behavior. For low diameters, where the transverse wall is found, the system behaves effectively one dimensional and in the limit $d\rightarrow 1$ the domain wall mobility follows Eq. (3). With increasing the diameter, the observed width of the transverse domain wall increases little due to the dipolar interaction, leading to small deviations from the analytic Slonczewski result assuming a Bloch wall width. Nevertheless, we confirmed numerically that Eq. (3) is still valid when the Bloch wall width Δ_B is replaced by the actual (numerically determined) width of the transverse wall.

Increasing the diameter of the system, a crossover from the transverse to the vortex wall is observed with a drastic increase of the domain wall mobility. As seen in Fig. 2, the reason for this effect is not a comparably drastic change of the wall width. Instead, as we will discuss in the following, for a vortex wall the domain wall mobility follows a law with a different dependence on the damping constant, namely, the Landau-Lifshitz formula,[4]

$$\frac{dv}{dB}=\frac{\gamma}{\alpha}\Delta, \tag{5}$$

where in our case Δ is the actual domain wall width of the vortex wall. The above equation is a limit of the more general Walker equation,[6–8]

$$v=\frac{\gamma Ba}{\alpha}\sqrt{\frac{J}{2(D_e+D_h\ \sin^2\phi)}}, \tag{6}$$

which was derived for sufficiently small driving fields for a system with an additional hard-axis anisotropy D_h. This anisotropy forces the equilibrium magnetization into an easy plane. Walkers formula is valid as long as the spin motion takes place in one plane, which is defined by a constant angle ϕ to the easy plane of the system. ϕ is given as

$$\sin\phi\cos\phi=\frac{\mu_s B}{\alpha 2 D_h}, \tag{7}$$

where this equation also defines a condition for the validity of the walker formula. For a given α there exists a maximum field value (or vice versa, for a given field a minimum α value) beyond which the spin motion is no longer restricted to one plane and instead an irregular precessional motion starts.[6] Note, that the Landau-Lifshitz formula is the $\phi=0$ limit of the Walker equation, i.e., the limit of a strong hard-axis anisotropy which forces the spin motion into the easy plane.

The above equations were derived for one-dimensional systems and the question arises why these formulas should be valid for the motion of a vortex wall with a nonuniform spin structure in cross-sectional planes. For a qualitative understanding, we note that the motion of the spins within each spin chain which is parallel to the wire axis is indeed restricted to a certain plane passing through the spins positions. For a spin chain at the surface of the cylinder, and in the limit of small driving fields, these are tangential planes of the cylinder surface. The responsible force that keeps the spin motion of each chain in this plane is for a vortex wall not a hard-axis anisotropy—as in the original calculation—but the energetical principle that forms the vortex, i.e., the combination of exchange and dipolar interaction. Since this is the condition under which Walkers formula was derived, it seems plausible that Eq. (6) describes the wall mobility in the case of an extended spin system as long as the spin motion during the reversal takes place in one plane. For a transverse wall, on the other hand, the situation is different: the precession of the wall leads to the fact that the motion of each single spin consists of precession and relaxation with no restriction to one single plane. These two different paths for the reversal of a spin are sketched in Fig. 4.

The main difference between Eqs. (3) and (5) is the dependence on damping. This is demonstrated in Fig. 5 which shows the ratio of the calculated wall mobility and the numerically determined domain wall width for two different strengths of dipolar interaction, leading to the two different wall shapes. In the high-damping limit both formulas agree. For a transverse wall the mobility shows a maximum at $\alpha=1$ and for lower damping the domain wall mobility decreases with decreasing damping constant. In the limit $\alpha\rightarrow 0$, only a precession of the domain wall remains without an effective wall motion along the wire.

For a vortex wall the domain wall mobility increases with decreasing damping constant following a $1/\alpha$ law as long as one is above a critical value α_c. As was discussed in connection with Eq. (7), this value α_c sets the limit of pure relaxational spin motion. As was discussed before, the role of the hard-axis anisotropy D_h in Eq. (7) in our case is played

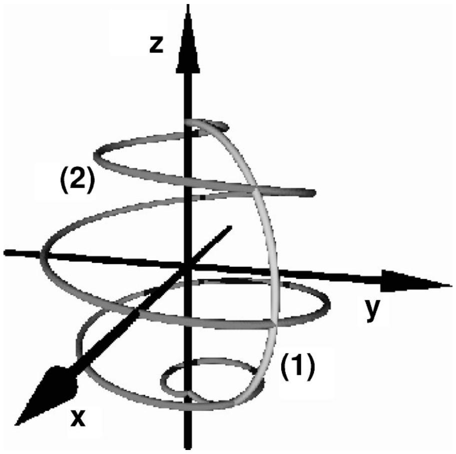

FIG. 4. Two different paths for the reversal of a spin. While (2) is dominated by precession, as in a transverse wall, path (1) is restricted to one plane as in a vortex wall.

by the combination of exchange and dipolar interaction, which forms the vortex and forces the spin motion into one plane. We would like to stress that for experimental systems the low-damping limit is more relevant. Here, the difference between the two domain wall mobilities (reduced to the domain wall width) can be extremely large, up to a factor of $1/\alpha^2$.

For smaller values of α below the critical one, the mobility decreases again and finally converges to a finite value since even for $\alpha=0$ the wall can move. In this limit the LLG equation conserves the energy of the system, and lowering the Zeeman energy leads to an increase of exchange energy, leaving an excited spin system behind the wall. These observations are also in agreement with the calculations of Schryer and Walker.[6]

This effect is demonstrated in Fig. 6. Here, profiles of the moving walls are shown as well as the so-called winding number

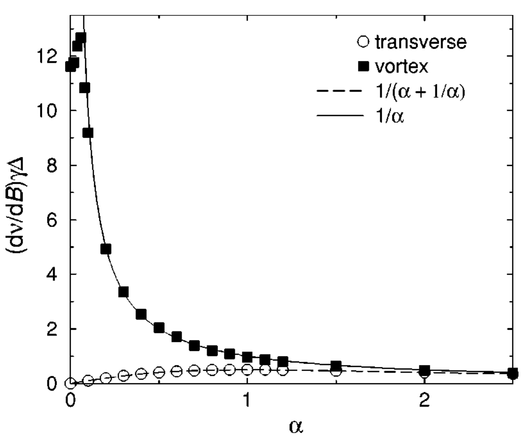

FIG. 5. Reduced domain wall mobility vs damping constant. The model parameters are $\omega/J=0.01$ (transverse wall) and $\omega/J=0.7$ (vortex wall), respectively, $D_e/J=0.05$, $\mu_s B/J=0.05$, $d=4$. Error bars are smaller than the symbol size.

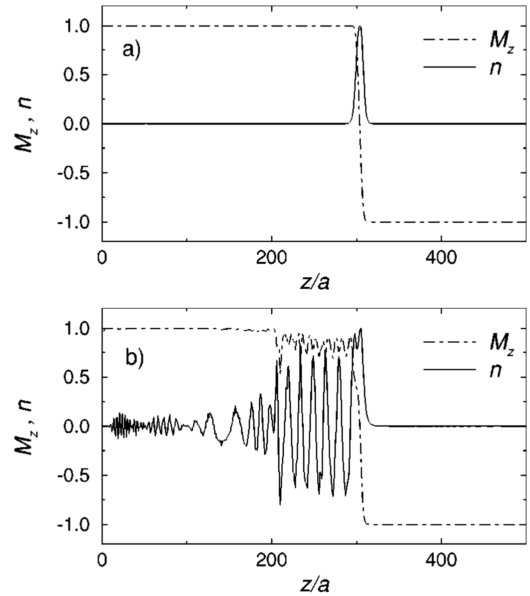

FIG. 6. Profiles and winding numbers of moving vortex walls in (a) the high-damping limit ($\alpha=1$) and (b) the low-damping limit ($\alpha=0$). $d=8$, $\omega/J=0.2$, $D_e/J=0.05$, $\mu_s B/J=0.1$.

$$n=\frac{1}{2\pi R}\int(\mathrm{rot}\,\mathbf{S})_z dx dy,$$

which is calculated numerically over all perpendicular planes of the wire. The winding number is a measure for the existence of vortices. $n=1$ means that all spins along the boundary are aligned building a ring with perfect flux closure. Figure 6 (a) shows the high-damping limit with a perfect vortex in the center of the wall. In the very low-damping limit Fig. 6(b), the situation is much more complicated. Here, behind the moving wall (smaller z) an excited spin system is left with vortex-type spin waves, which are ejected from the moving wall.

To conclude, in agreement with prior work[10,12,13] we have found different wall structures for driven domain walls in cylindrical systems, transverse and vortex walls, depending on the diameter of the system as compared to the exchange length of the given material. While for vortex walls the domain wall velocity is described by the formula from Walker, transverse walls follow a formula from Slonczewski. In both cases the domain wall velocity is proportional to the domain wall width. The main difference is the dependence on the damping constant. For small values of the damping constant this difference can lead to drastic differences where the velocity of the vortex wall is up to a factor of $1/\alpha^2$ larger. The reason for this difference is probably the fact that each spin motion in the case of the vortex wall is completely within one single plane as is the case for the model where the Walker formula was derived for, while this is not the case for a transverse wall where the precession of the wall leads to a three-dimensional spin motion.

The authors thank D. Garanin and S. Lübeck for helpful discussions. This work was supported by the Deutsche Forschungsgemeinschaft (Grant Nos. SFB 491 and NO290).

[1] C.A. Ross, R.W. Chantrell, M. Hwang, M. Farhoud, T.A. Savas, Y. Hao, H.I. Smith, F.M. Ross, M. Redjdal, and F.B. Humphrey, Phys. Rev. B **62**, 14 252 (2000).
[2] K. Nielsch, R.B. Wehrspohn, J. Barthel, J. Kirschner, S.F. Fischer, H. Kronmüller, T. Schweinböck, D. Weiss, and U. Gösele, J. Magn. Magn. Mater. **249**, 234 (2002).
[3] T. Ono, H. Miyajima, K. Shigeto, K. Mibu, N. Hosoito, and T. Shinjo, Science **284**, 468 (1999).
[4] D.L. Landau and E. Lifshitz, Phys. Z. Sowjetunion **8**, 153 (1935).
[5] A.P. Malozemoff and J.C. Slonczewski, *Magnetic Domain Walls in Bubble Materials* (Academic Press, New York, 1979).
[6] N.L. Schryer and L.R. Walker, J. Appl. Phys. **45**, 5406 (1974).
[7] J.F. Dillon, in *Magnetism*, edited by G.T. Rado and H. Suhl (Academic Press, New York, 1963), Vol. 1, p. 149.
[8] D.A. Garanin, Physica A **178**, 467 (1991).
[9] U. Nowak, in *Annual Reviews of Computational Physics IX*, edited by D. Stauffer (World Scientific, Singapore, 2001), p. 105.
[10] D. Hinzke and U. Nowak, J. Magn. Magn. Mater. **221**, 365 (2000).
[11] A. Hubert and R. Schäfer, *Magnetic Domains* (Springer-Verlag, Berlin, 1998).
[12] H. Forster, T. Schrefl, D. Suess, W. Scholz, V. Tsiantos, R. Dittrich, and J. Fidler, J. Appl. Phys. **91**, 6914 (2002).
[13] R. Hertel, J. Magn. Magn. Mater. **249**, 251 (2002).